Supporting Information for

Manipulating and Probing the Distribution of Excess Electrons in an Electrically Isolated Self-Assembled Molecular Structure

Philipp Scheuerer, Laerte L. Patera, and Jascha Repp

Institute of Experimental and Applied Physics, University of Regensburg, Regensburg 93053, Germany

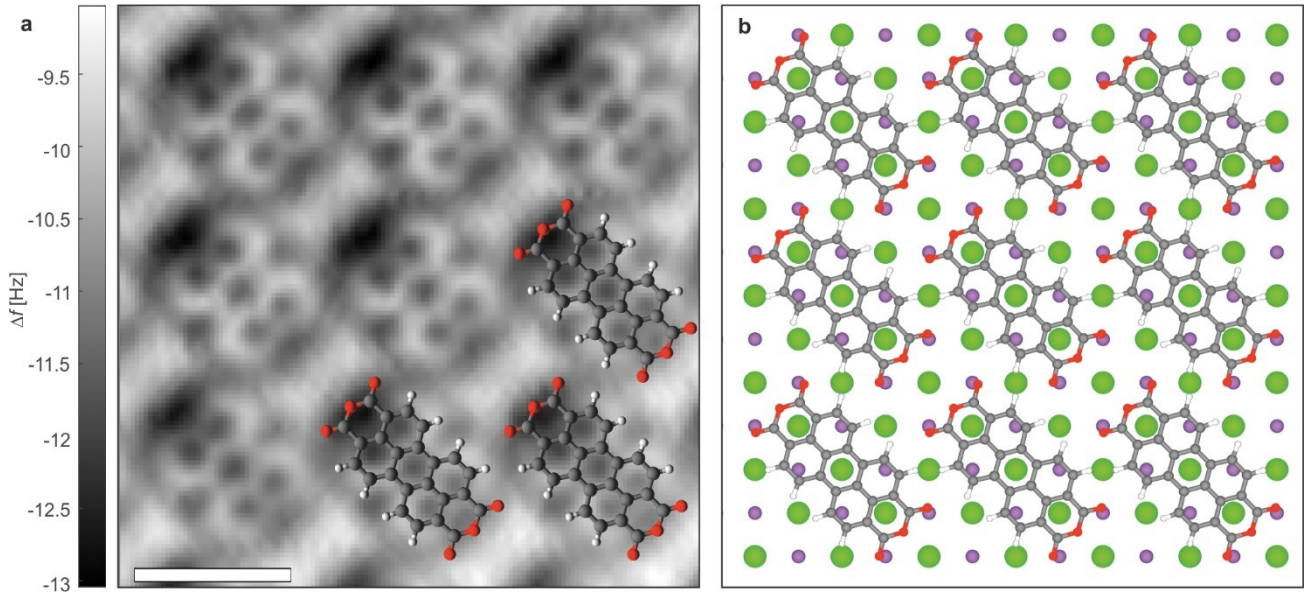

Figure S1. (a) High-resolution AFM image with a CO-functionalized tip of a part of a large PTCDA island on NaCl(2ML)/Au(110). For comparison, molecular structures are superimposed in the AFM image. The scalebar corresponds to 10 Å. Setpoint: 0.05 V, 2.8 pA, z-offset: 1.9 Å. The scalebar corresponds to 10 Å. (b) Adsorption geometry model of PTCDA/NaCl. Na^+ (purple), Cl^- (green), carbon (grey), oxygen (red) and hydrogen (white).

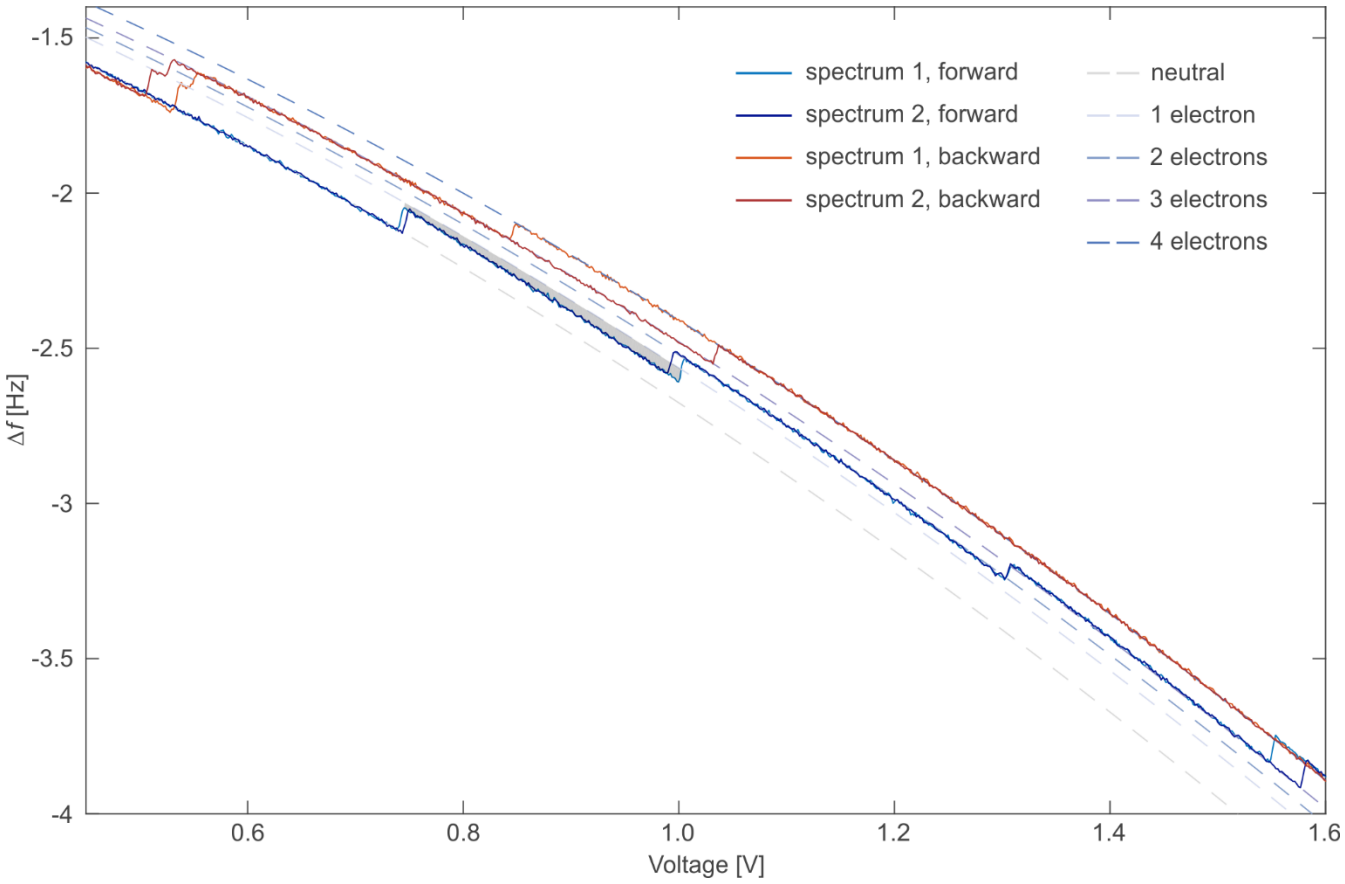

Figure S2. Charge-state analysis of spectra showing multiple charging. Zoom-in of the spectrum shown in Fig 1b (spectrum 1) and a subsequently recorded spectrum under the same conditions (spectrum 2) showing the first four charge-state transitions. The feedback loop was not activated between acquisition the two spectra. The dashed curves indicate the Kelvin parabolas of the distinct charge states. The one corresponding to the neutral state was obtained from a parabolic fit of the Δf signal in the neutral region. The others are horizontally offset with respect to the latter fit. The deviation of the Δf spectra for $N = 1$ in the forward direction highlighted as a grey area can be attributed to the simultaneous occurrence of dissipation (not shown), arising from tip induced charge transfer. The spectra demonstrate the excellent reproducibility of the charging and discharging behavior and allow for an assignment to charge states. The discharging events $3^- \rightarrow 2^-$, $2^- \rightarrow 1^-$ and $1^- \rightarrow 0$ do (almost) collapse on a single step. This can be qualitatively rationalized as follows. For $N = 2$ and 3 the charges will localize outside the center of the island and are therefore only very weakly tunnel coupled to the tip that is located above the center of the island. For these transitions discharging occurs therefore shifted to much lower voltages. In contrast, the last electron is located at the center of the molecule and can be extracted much more easily to the tip.

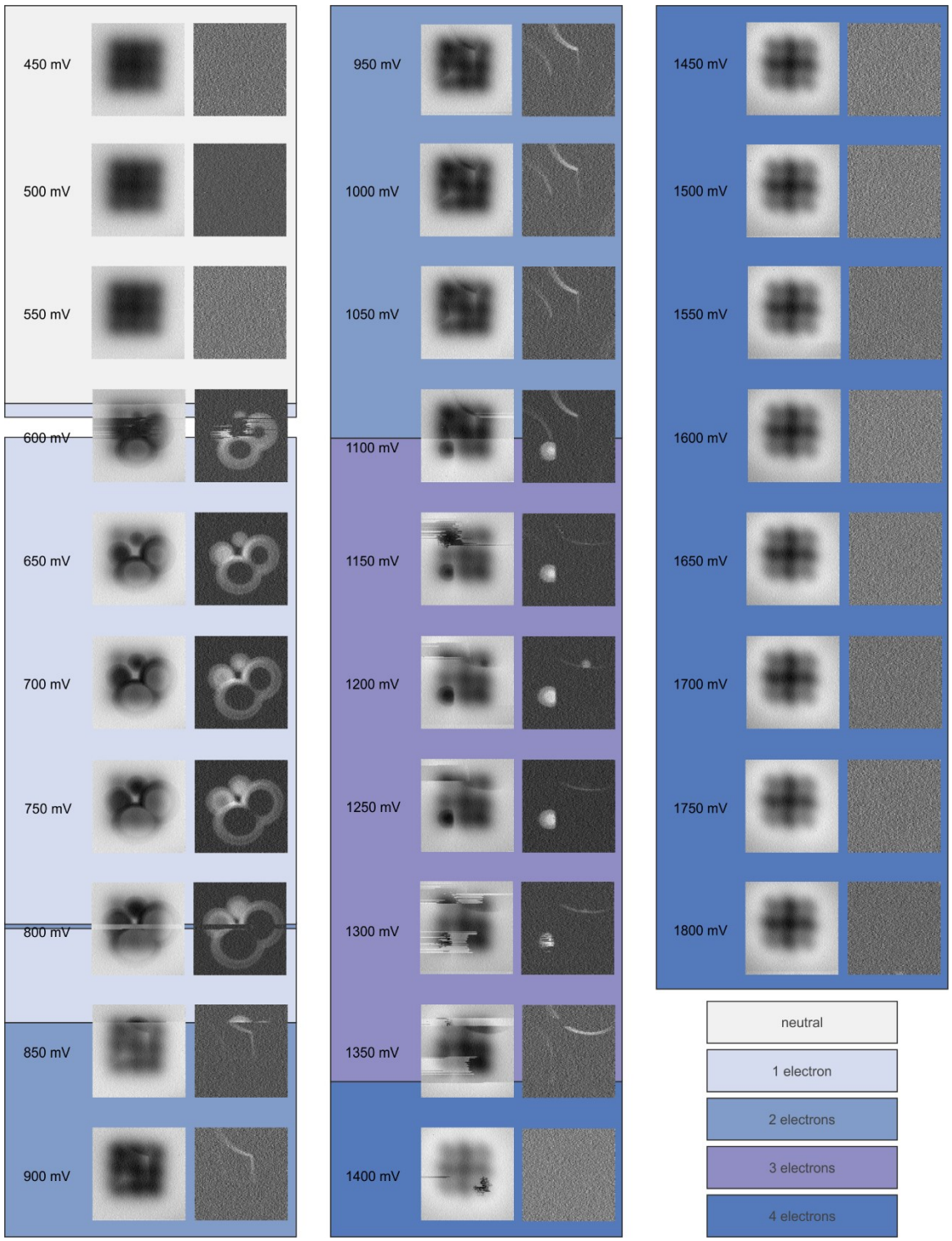

Figure S3. Full set of AFM images at different bias voltages. The background colors indicate the island charge state (see bottom right legend). Charge-state transitions are clearly visible as a sharp contrast change in the Δf channel during image acquisition. Setpoint: Δf = -1.3 Hz at V = 0.0 V, A = 1 Å, z-offset: 3 Å.

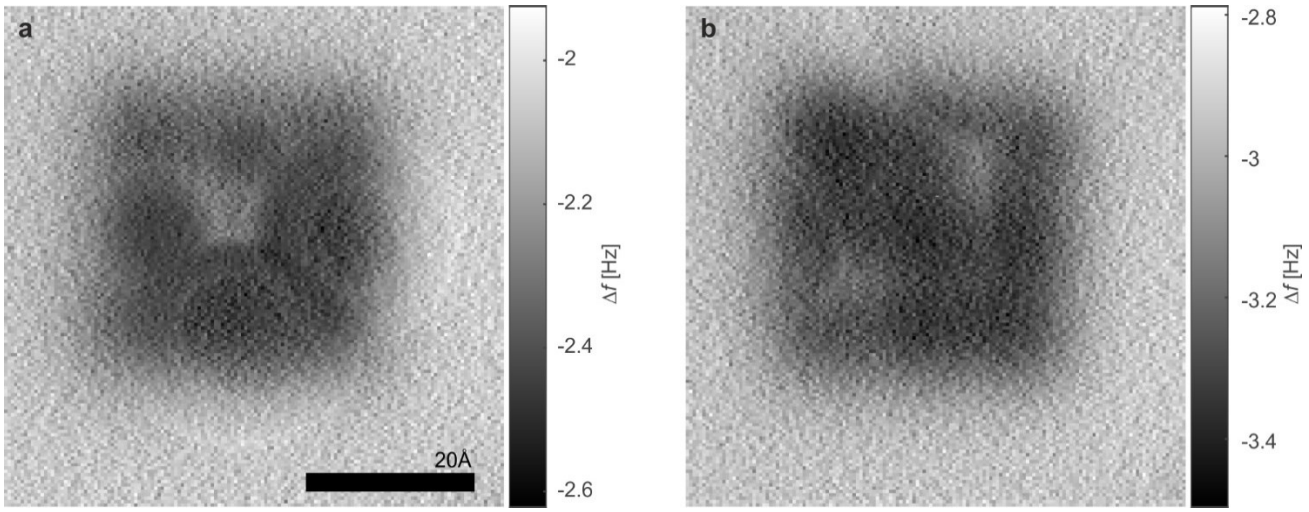

Figure S4. AFM images of the 3-by-3 island hosting one (a) and two (b) excess electrons after subtraction of the Δf contrast attributed to the intermolecular charge transfer. To achieve this, the fixed ratio between frequency change and dissipation rate due to intra-island tunneling was exploited (see also Figure S6). The background-subtracted dissipation signal was converted to a dissipation rate in units of Hz[37] and multiplied with a scaling factor s = 0.12 providing the frequency change due to intra-island tunneling, which finally was subtracted from the original images. Thus, in the resulting images a brighter Δf contrast should indicate that the excess charge is localized beneath the tip. (a) The image contrast for a single excess electron shows a bright feature at the center in agreement with the ground-state configuration hosting the excess electron at the center. The absence of any bright feature at the edge molecules indicates that in the charge configuration influenced by the tip's potential, the excess charge is not being pulled to below the tip, but rather pushed away. (b) For two excess electrons the contrast at two opposing corners is brighter, indicating that the two excess electrons preferentially occupy those two corner molecules in the ground state configuration. Also here, the charge configurations that are influenced by the tip's potential do not feature the excess charge being transferred to below the tip.

Model and parameterization

We modelled the electron distribution in the island as a function of bias voltage and tip position as described in the methods section of the main text. The pair-wise Coulomb interaction from the mutual repulsion of the electrons dominates the energy separation of the sequential charging steps. On the scale of this energy spacing (≈ 0.2 eV), the energy difference between the different sites, center, edge and corner are minor. Therefore, the effective dielectric constant ε that accounts for the screening due to the environment can be reliably fit from this spacing such that the voltage difference between the $0 \rightarrow 1^-$ and the $3^- \rightarrow 4^-$ transitions matches the value of the experiment of ≈ 0.75 V. Taking the relative voltage drop inside the NaCl film of ≈ 30% into account sets ε to 4. Further, the charge state $N = 2$ was inferred from the experiment to have the two excess electrons in two opposing corners of the island. Using the previously determined value of ε = 4, the Coulomb repulsion between the electrons is calculated to energetically favor this configuration by 46 meV as compared to another configuration, in which the two electrons are located in two opposing edge molecules. As the former is found to be indeed the ground state, this energy difference must outweigh twice the energy difference of the LUMO for edge as compared to corner sites and thereby sets an upper bound for the latter. Conversely, the difference in charging voltages for the first excess charge injection at the center, edge and corner molecules (main text, Figure 2) shows that this energy difference should not be much smaller than 20 meV. We therefore set the energy difference between center and edge molecules to 32 meV and the one between edge and corner molecules to 20 meV in the simulation. These are the most important fit parameters that from the above considerations are set with a relative confidence interval of about ± 30%. With these, the energetic levels for different configurations as shown in Figure 4 were simulated, while (i) variations of the background potential, (ii) the energy difference of non-equivalent corner molecules and (iii) the potential of the tip were not considered.

Beyond this, the simulations are not meant to claim any quantitative description of the tip or other, more detailed parameters. To nevertheless better understand the patterns observed in the dissipation signal, the aforementioned three components (i-iii) were included into the model to also simulate the influence of the lateral tip position. The tip potential was modelled as a combination of an electric monopole and dipole located at the tip position, which was assumed to be 10 Å above the molecular plane. To fit the experimentally observed patterns it had to be assumed that the tip's dipole field acting on the molecules directly, indirectly also affects all nearest neighbors. Hence, any energetic shift arising from the tip's dipole calculated for a certain molecule was assumed to also shift all neighbors of that molecule with a certain scaling factor. This may be rationalized by the interaction of neighboring molecules via the intermolecular O···H bridges. The deviation from the system's C_{2v} symmetry in the damping image for one excess electron could be accounted for by assuming a tilt of the background potential of only 3.5 meV/nm. While this specific value depends on other model parameters and cannot be considered as reliable, it provides the order of magnitude of such fluctuations and yields some insight, how critically the charge distribution can be affected. With these prerequisites, the energetically favored charge configuration was calculated for all lateral tip positions and plotted in Figure S5. At the transitions from one configuration to another one, a near degeneracy of two configurations is expected, such that the vertical oscillation of the tip can repeatedly tip the energy balance, in turn giving rise to intra-island charge transfer and potentially a dissipation signal. Note, that if the transition between such two nearly degenerate configurations requires not just an electron transfer between two neighboring molecules but transfers of multiple electrons or over larger distances, the transition rate will probably be too low to be observable as a dissipation signal.

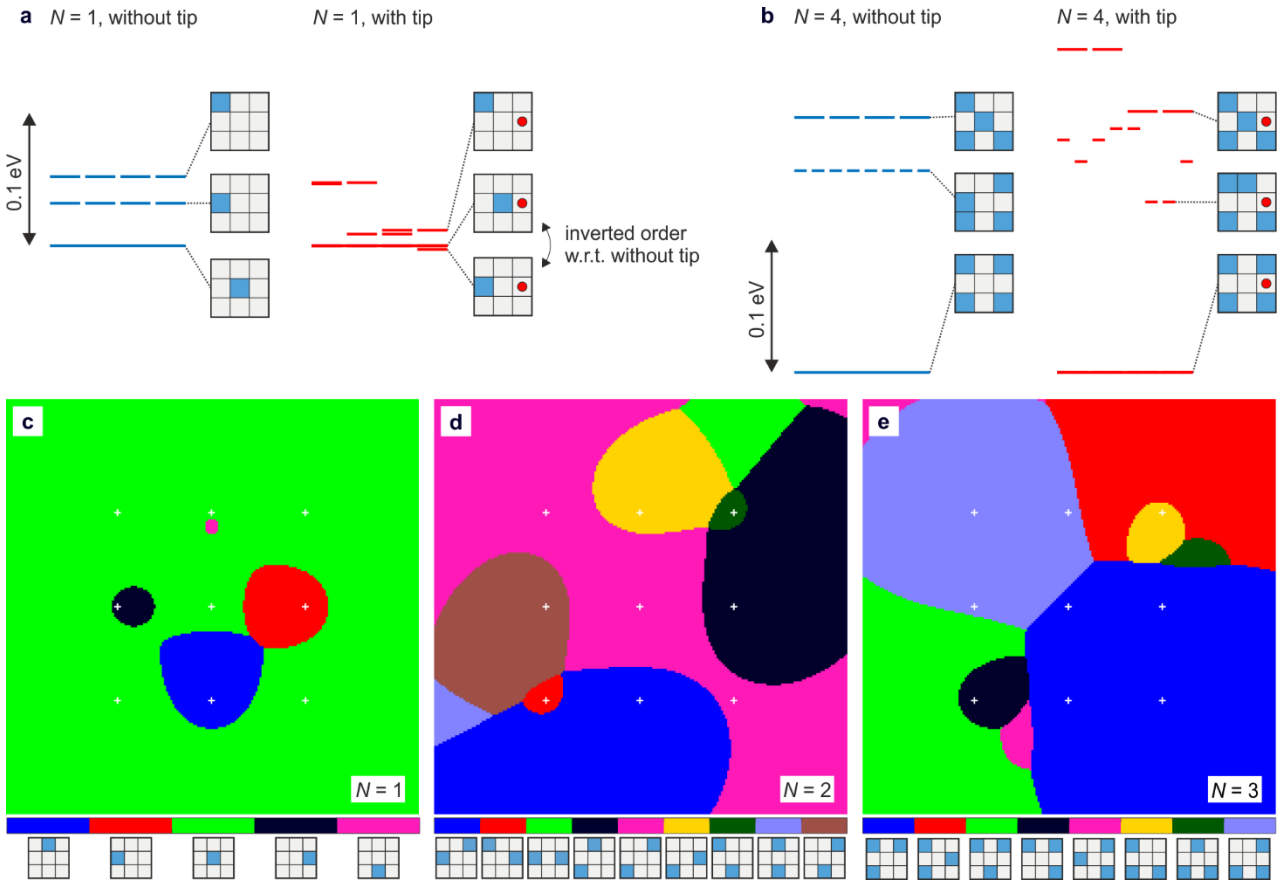

Figure S5. Simulated dependence of level alignment and electron configurations on the lateral tip position for one and four electrons. (a) Level alignment for one excess electron ($N = 1$) within the island with and without the influence of the tip. Exemplarily, the tip position is simulated to be above the rightmost edge molecule and indicated by a red dot in each schematic representation of the configurations. For $N = 1$ the influence of the tip is strong enough to stabilize the excess electron in an edge molecule opposite to the tip position. (b) In contrast, for $N = 4$ the level sequence does not change in presence of the tip, such that only a single configuration with the four electrons in corner molecules is favored. (c-e) Dependence of electron configurations from lateral tip position for one (c), two (d) and three (e) excess charges. Distinct colors indicate the areas corresponding to a certain favorable charge configuration. For the simulations shown in (c-e) we introduced a potential background tilt of 3.5 mV/nm in the simulations to account for the asymmetries observed in experiments. Such asymmetries could arise from the surrounding (defects, step edges, other islands). Further, an energy difference of non-equivalent corner molecules was included in the simulation as fit parameter. Crosses indicate positions of the molecules. The charge configuration corresponding to the colors are assigned below each image. Note that, for the energy schemes in (a) and (b) the corner energy difference and the aforementioned potential background tilt were set to zero, in order to reflect the expected degeneracies.

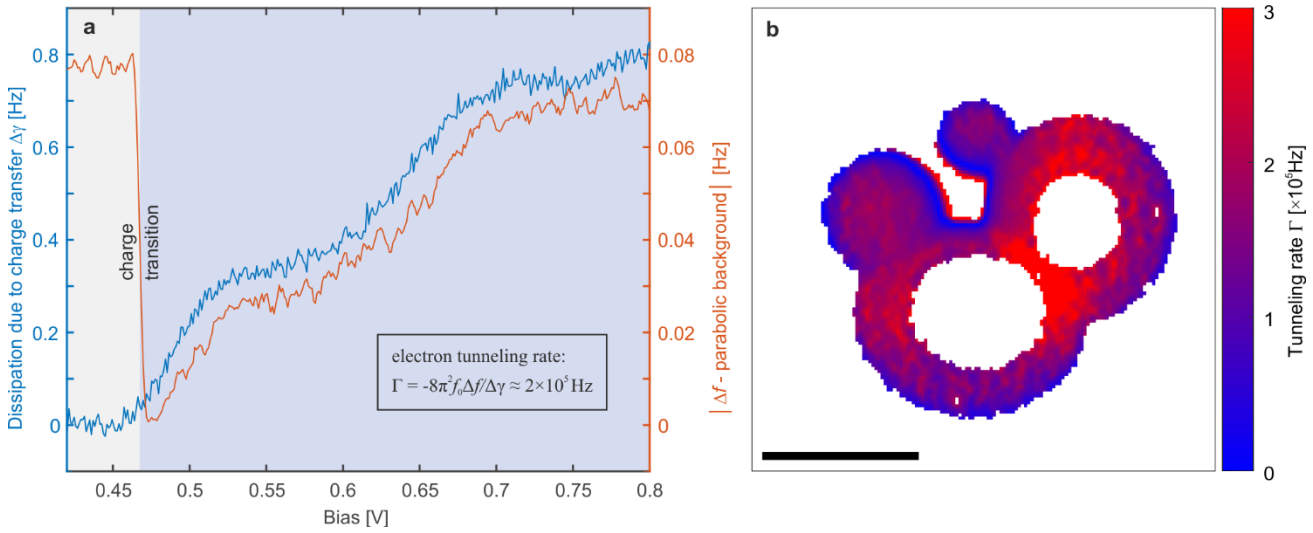

Figure S6. Relation between frequency change and dissipation rate due to intra-island tunneling and the resulting tunneling rate. If electron tunneling is driven by the cantilever motion and leads to a signal in frequency shift and dissipation, following reference[38] the electron tunneling rate Γ can be determined from the ratio of Δf, the frequency shift arising from this process, divided by $\Delta\gamma$, the additional dissipation rate[37], as $\Gamma = -8\pi^2 f_0 \Delta f/\Delta\gamma$, where f_0 denotes the free-cantilever resonance frequency. The conversion of a dissipation signal to a dissipation rate is performed by relating it to the cantilever's intrinsic damping, for which the dissipation rate is set by the quality factor Q of the cantilever. This results in the equation $\Delta\gamma = (2\pi f_0/Q)(A_{\mathrm{exc}} - A_{\mathrm{exc0}})/A_{\mathrm{exc0}}$, where A_{exc0} is the background dissipation signal and A_{exc} the total dissipation.[37] (a) From the data displayed in Fig. 2a, $-\Delta f$ and $\Delta\gamma$ were extracted by subtracting the parabolic background[34] and intrinsic dissipation rate,[37] respectively. Obviously, there is a linear scaling between $-\Delta f$ and $\Delta\gamma$, which yields a constant intra-island tunneling rate $\Gamma \approx 2\cdot10^5$ Hz. (b) Similarly, the intra-island tunneling rates Γ can be extracted from images. Here the image displayed in Fig. 3b is used, and similar tunneling rates in the range of $2\cdot10^5$ Hz are obtained. Note that, the apparent lateral variation of the rates might be due to the different bandwidth of the two signals Δf and $\Delta\gamma$. The similar rates obtained from (a) and (b) under very different conditions support our assignment as intra-island tunneling. Note that, the tunneling rates are not only governed by the overlap of the electronic wave functions, but also by the Franck-Condon factors associated to the nuclear displacement (polarization) upon charge transfer.